BULLETIN OF THE POLISH ACADEMY OF SCIENCES
TECHNICAL SCIENCES, Vol. 73(6), 2025, Article number: e155889
DOI: 10.24425/bpasts.2025.155889

Comparison of calculation times of FOPID and PID controllers along with control quality for Two Rotor Aerodynamical System

Jakub ŻEGLEŃ-WŁODARCZYK*

AGH University of Krakow, Poland

Abstract. Two Rotor Aerodynamical System can be compared to a tethered helicopter. This is one of the systems in which the problem of cross-coupling occurs, which complicates the implementation of control. Therefore, in the case of TRAS system, four controllers are most often used. PID and FOPID controllers were used in different configurations in order to compare them. First, coefficients were selected using the Grey Wolf Optimizer algorithm. Then, based on simulation, a preliminary comparison of the controllers was made. In the next part, measurements were carried out on the real device. Based on the cost function, it was noticed that FOPID controllers achieve better results. In the case of FOPIDs, there may be concerns related to the calculation time. This is a valid question related to the possible application of this type of control for devices requiring control determination in real time. Therefore, the calculation times of the individual controllers were also measured and compared.

Keywords: Two Rotor Aerodynamical System; TRAS; Grey Wolf Optimizer; PID; FOPID; calculation time; real time requirements.

1. INTRODUCTION

Air transport in terms of control is a rather complex problem due to the fact that the flight takes place in three-dimensional space. It is worth mentioning here helicopters, which have the ability to take off and land vertically. This allows reaching more places than in the case of airplanes, which need a long, specially prepared runway. One can read more about helicopter dynamics in [1]. Reduced versions of helicopters to an unmanned form are drones. Just like helicopters, they can stay in one specific place in the air, which makes it easier, among other things, to take photos [2, 3] and make all kinds of measurements [4, 5]. This paper focuses on the Two Rotor Aerodynamical System (TRAS), which can be considered a miniaturized version of a tethered helicopter.

TRAS is a multi-input, multi-output nonlinear dynamic system [6–8]. It is a good prototyping device because it is tethered. This means that in case of large control errors, destruction of the object can be avoided. The task of this device is to keep up with the given azimuth and pitch angles. This can only be controlled by the speed of the rotors, because the angle of attack of the rotors is constant. In addition, the phenomenon of cross-coupling can be observed in the system. In this case, it means that each of the rotors affects both angular values.

PID is one of the most popular controllers. Nicolas Minorsky wrote an article about it in 1922 [9]. Since then, it has been used more often due to its ease of implementation and robustness. PID is also frequently used as a reference when comparing controllers, e.g. [10–12].

Fractional order calculus is a generalization of integer-order calculus [13]. The assumption is as follows: the derivative does not have to be of integer order. Such operations require large computational powers, therefore the development of this branch of mathematics began to advance together with improvements of computers. The book [14] presents a lot of information on fractional calculus.

In order to find the controller coefficients, it is worth using heuristic optimization algorithms, such as Grey Wolf Optimizer (GWO) [15], Whale Optimization Algorithm (WOA) [16] or Particle Swarm Optimization (PSO) [17]. These types of algorithms can search large spaces and find optimal or suboptimal solutions quite quickly.

Other articles indicate that GWO can be successfully used to optimize FOPID controllers. This is evidenced by simulation comparisons in [18]. GWO was also used in [19] in order to optimize FOPID controllers in grid-tied photovoltaics system. Simulations indicate very good performance in comparison to other methods. Therefore, in this article it was decided to use Grey Wolf Optimizer algorithm to determine FOPID coefficients. Testing of other methods is planned in subsequent articles.

In this preface, a short introduction to each topic was made. In the following part, more detailed information of the FOPID controller and the Grey Wolf Optimizer algorithm will be presented. The next part will focus on the mathematical model of the Two Rotor Aerodynamical System with the control implementation. Finally, the simulation responses and tests on a real object will be presented. In addition, the calculation times of the controllers will be compared. At the end, conclusions will be presented.

*e-mail: zeglen@agh.edu.pl

Manuscript submitted 2025-04-28, revised 2025-07-28, initially accepted for publication 2025-08-17, published in November 2025.

2. FOPID CONTROLLER

Fractional calculus is a generalization of differential and integral calculus to the fundamental operator ${}_aD_t^r$ of fractional order, where a and t are limits of the operation, and $r \in \Re$. The continuous integral-differential operator is defined as [20]:

$$ {}_aD_t^r = 3\begin{cases} \dfrac{\mathrm{d}^r}{\mathrm{d}t^r} & \text{when } r > 0, \\ 1 & \text{when } r = 0, \\ \displaystyle\int_a^t (\mathrm{d}\tau)^{-r} & \text{when } r < 0. \end{cases} \tag{1} $$

To numerically calculate the fractional derivative, one can use a very popular method, which is the Oustaloup Recursive Approximation. This is a recursive filter that very well approximates the fractional derivative [21]. The method is based on the approximation of the function of the form:

$$ H(s) = s^r \tag{2} $$

for the selected frequency range $\omega \in [\omega_b, \omega_h]$ by a rational function:

$$ \widehat{H}(s) = C_0 \prod_{k=-N}^{N} \frac{s+\omega_k'}{s+\omega_k}, \tag{3} $$

where $r \in \Re$, r is in the range $[-1, 1]$ and N is the order of approximation. The poles, zeros and gain of the filter can be determined using the formulas:

$$ \begin{aligned} \omega_k' &= \omega_b \left(\frac{\omega_h}{\omega_b}\right)^{\frac{k+N+0.5(1-r)}{2N+1}}, \\ \omega_k &= \omega_b \left(\frac{\omega_h}{\omega_b}\right)^{\frac{k+N+0.5(1+r)}{2N+1}}, \\ C_0 &= \left(\frac{\sqrt{\omega_h \omega_b}}{\omega_h}\right)^r \prod_{k=-N}^{N} \frac{\omega_k}{\omega_k'}. \end{aligned} \tag{4} $$

The generalization of the PID controller to fractional calculus is FOPID (fractional order PID). It has two additional parameters, which are non-integer orders of integration and differentiation. Therefore, the transfer function of the FOPID controller takes the following form [22, 23]:

$$ G_{\mathrm{FOPID}} = K_P + \frac{K_I}{s^\lambda} + K_D s^\mu, \tag{5} $$

where K_P, K_I, K_D remain unchanged with respect to PID, while λ is the order of the integral and μ is the order of the differentiation.

3. GREY WOLF OPTIMIZER

The Grey Wolf Optimizer algorithm is based on the behavior of grey wolves [15]. This method pays attention to two features of the pack. These are the hierarchy of animals and the hunting strategy. The pack can be divided into the following groups:

- alpha – leader,
- beta – main wolf helpers,
- delta – other activities, e.g., hunting, scouting,
- omega – the weakest units.

It is assumed that the best solution is provided by the alpha wolf, while the second and third best possibilities are considered to be beta and delta individuals. The remaining solutions are omega wolves.

During the hunt, wolves start to surround the prey, which can be described by the following equations [15]:

$$ D = |CX_p(t) - X(t)|, \tag{6} $$

$$ X(t+1) = X_p(t) - AD, \tag{7} $$

where $||$ is the absolute value, t denotes the current iteration, A and C are coefficients, X_p is the position of the prey, X is the position of the wolf. Vectors A and C are calculated as follows:

$$ A = 2ar_1 - a, \tag{8} $$

$$ C = 2r_2, \tag{9} $$

where a is linearly decreased from 2 to 0, r_1 and r_2 describe random numbers in the range $[0, 1]$.

The next step is to circle the victim. It is assumed that the alpha, beta and delta wolves have the best knowledge about the location of the victim. Therefore, the remaining omega individuals update their position based on the most important individuals. This is described by the following equations:

$$ \begin{aligned} D_\alpha &= |C_1 X_\alpha - X|, \\ D_\beta &= |C_2 X_\beta - X|, \\ D_\delta &= |C_3 X_\delta - X|, \end{aligned} \tag{10} $$

$$ \begin{aligned} X_1 &= X_\alpha - A_1 D_\alpha, \\ X_2 &= X_\beta - A_2 D_\beta, \\ X_3 &= X_\delta - A_3 D_\delta, \end{aligned} \tag{11} $$

$$ X(t+1) = \frac{X_1 + X_2 + X_3}{3}, \tag{12} $$

where X_1, X_2, X_3 define the alpha, beta and delta location vectors.

Approaching the prey in order to attack it is represented by decreasing the value of a. In addition, A is also dependent on a and $r1$ belonging to the interval $[-1, 1]$. Finally, if $|A| < 1$, it means that the wolves try to move towards the prey.

4. MATHEMATICAL MODEL

Two Rotor Aerodynamical System consists of two beams. One is vertical and stationary. The other is placed halfway up on top of the first. Two rotors are mounted at both ends of the horizontal pole, perpendicular to each other, as in helicopters. The angle of attack of the propellers is constant, so the aerodynamic forces can only be controlled by the speed of the rotors. Sensors are

also installed to measure the azimuth and pitch angles. It should be noted that TRAS is a system in which the phenomenon of cross-coupling occurs. In this particular case, this means that each of the rotors affects both values of the measured angles. TRAS is classified as a nonlinear MIMO system. An example of the laboratory version of the TRAS device is shown in Fig. 1. More information about the mathematical model can be found in the manual [6] and many other articles, e.g., [7, 8].

Fig. 1. Two Rotor Aerodynamical System

In order to determine the mathematical model, the following assumptions were made [6]:

- The dynamics of the propeller subsystem can be described by first-order differential equations.
- The friction in the system is of the viscous type.
- The propeller-air subsystem can be described in accordance with the postulates of the flow theory.

The following notations were adopted:

J_v – sum of moments of inertia relative to the horizontal axis
J_h – sum of moments of inertia relative to the vertical axis
α_v – pitch angle of the beam
α_h – azimuth angle of the beam
Ω_h – angular velocity of the beam around the vertical axis
Ω_v – angular velocity around the horizontal axis
ω_v – angular velocity of the main rotor
ω_h – angular velocity of the tail rotor
$F_v(\omega_m)$ – dependence of the propulsive force on the angular velocity of the rotor
$F_h(\omega_t)$ – dependence of the propulsive force on the angular velocity of the tail rotor
f_v – friction coefficient in the horizontal axis
f_h – friction coefficient in the vertical axis
U_h – horizontal DC-motor PWM control input
U_v – vertical DC-motor PWM voltage control input
M_h – horizontal turning torque
K_h – horizontal angular momentum
K_v – vertical angular momentum
m_t – mass of the tail part of the beam
m_{tr} – mass of the tail motor with tail rotor
m_{ts} – mass of the tail shield
m_m – mass of the main part of the beam
m_{mr} – mass of the main DC-motor with main rotor
m_{ms} – mass of the main shield
m_b – mass of the counter-weight beam
m_{cb} – mass of the counter-weight
l_t – length of the tail part of the beam
l_m – length of the main part of the beam
l_b – length of the counter-weight beam
l_{cb} – distance between the counter-weight and the joint
r_{ms} – radius of the main shield
r_{ts} – radius of the tail shield
k_{hv} – constant
k_{vh} – constant
a_1 – constant
a_2 – constant

Ultimately, Two Rotor Aerodynamical System can be described by the following equations:

$$\frac{d\omega_v}{dt} = \frac{l_m F_v(\omega_m) - \Omega_v K_v + g((A-B)\cos\alpha_v - C\sin\alpha_v)}{J_v} \cdots \frac{-\frac{1}{2}\Omega_h^2 (A+B+C)\sin 2\alpha_v U_h k_{hv} + U_h k_{hv} - a_1 \Omega_v abs(\omega_v)}{J_v} \tag{13}$$

$$\frac{\mathrm{d}\alpha_v}{\mathrm{d}t} = \Omega_v\,, \tag{14}$$

$$\frac{\mathrm{d}K_h}{\mathrm{d}t} = \frac{M_h}{J_h} = \frac{l_t F_h(\omega_t)\cos\alpha_v - \Omega_h K_h + U_v k_{vh}}{D\sin^2\alpha_v + E\cos^2\alpha_v + F} \cdots \frac{-a_2 \Omega_h abs(\omega_h)}{D\sin^2\alpha_v + E\cos^2\alpha_v + F}\,, \tag{15}$$

$$\frac{\mathrm{d}\alpha_h}{\mathrm{d}t} = \Omega_h = \frac{K_h}{J_h \alpha_v}\,, \tag{16}$$

where

$$A = \left(\frac{m_t}{2} + m_{tr} + m_{ts}\right) l_t\,,$$
$$B = \left(\frac{m_m}{2} + m_{mr} + m_{ms}\right) l_m\,,$$
$$C = \left(\frac{m_b}{2} l_b + m_{cb} l_{cb}\right),$$

$$D = \frac{m_b}{3} l_b^2 + m_{cb} l_{cb}^2,$$

$$E = \left(\frac{m_m}{3} + m_{mr} + m_{ms}\right) l_m^2 + \left(\frac{m_t}{3} + m_{tr} + m_{ts}\right) l_t^2,$$

$$F = m_{ms} r_{ms}^2 + \frac{m_{ts}}{2} r_{ts}^2.$$

5. IMPLEMENTATION

The control system was prepared in the MATLAB/Simulink environment, which is shown in Fig. 2. The grey block in the center symbolizes the TRAS model. It has two inputs, which are the control for the main rotor and the control for the tail rotor. In addition, four outputs are distinguished: azimuth angle, pitch angle, azimuth velocity and pitch velocity. The angular values are sent through negative feedback loops and compared with the reference. Then the differences go as input to the controllers, which are located in the *FOPID Controllers* block.

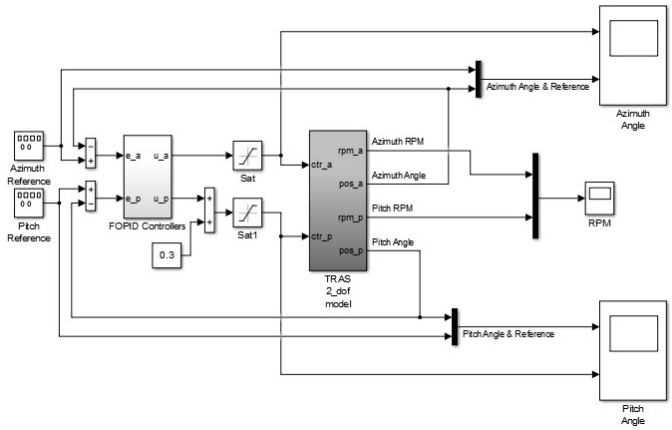

Fig. 2. Simulation model of Two Rotor Aerodynamical System

It should be assumed that:

e_a – difference between the set value and the current value of the azimuth angle,

e_p – difference between the set value and the current value of the pitch angle.

The following control variants were proposed:

Variant 1 – four PID controllers – Fig. 3.

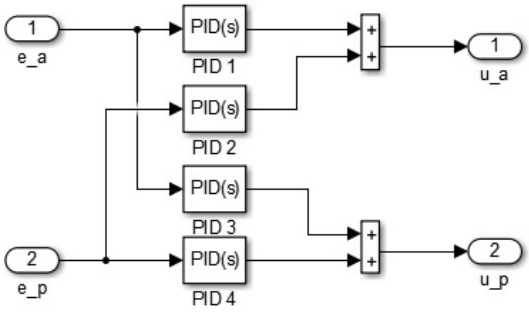

Fig. 3. First control variant

Variant 2 – two PID controllers and two FOPID controllers – Fig. 4.

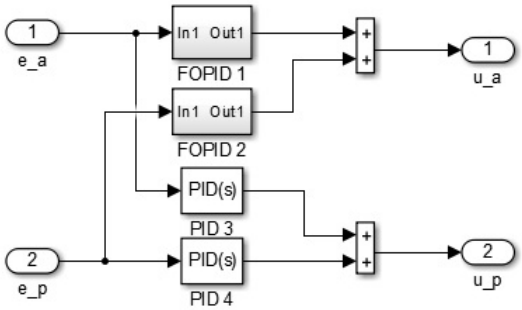

Fig. 4. Second control variant

Variant 3 – four FOPID controllers – Fig. 5.

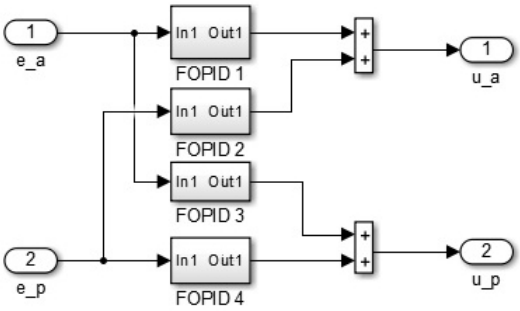

Fig. 5. Third control variant

It should be noted that in all variants parallel control was used, differing in the number of PIDs and FOPIDs. The value e_a is sent to controllers numbered 1 and 3. On the other hand, e_p is sent to controllers numbered 2 and 4. In the next part, two values calculated by the controllers are added up. Each of them had different deviation values (e_a and e_p) given at the input. In this way, both control values use information about the azimuth angle and the tilt angle.

It was decided to use the GWO algorithm for optimization. The process immediately gave satisfactory results. Therefore, it was decided to continue research using it. For optimization algorithm the following cost function was defined:

$$J = \int_0^\infty \left(|e_a(t)| + |e_p(t)|\right) \mathrm{d}t. \tag{17}$$

Additionally, the following inputs (Table 1) and initial range of individual coefficients were used (18).

Table 1
Input values for the Grey Wolf Optimizer algorithm

Parameter	Value
Number of wolves	5
Maximum number of iterations	200

$$\begin{aligned} K_P &= [0:50], \\ K_I &= [0:50], \\ K_D &= [0:50], \\ \lambda &= [0:1], \\ \mu &= [0:1]. \end{aligned} \tag{18}$$

6. RESULTS

Due to the fact that the entire system is tethered (which is also visible in Fig. 1), no tests related to the vertical take-off and landing were performed. The following test scenario was used:

- Sudden changes in the azimuth angle between −0.8 rad and 0.8 rad (and vice versa) every 20 seconds.
- Gradual sinusoidal changes in the pitch angle with an amplitude of 0.3 rad and a period of 30 seconds.

The controller coefficients were selected after conducting many simulations using Grey Wolf Optimizer algorithm with cost function (17). Their values are presented in Table 2. The numbering of individual controllers is identical to Figs. 3–5. In order to use the FOPID controllers, it was decided to use Oustaloup Recursive Approximation. The order of approximation was 8. The frequency was in range $\omega \in [10^{-3}, 10]$. More information about research can be found in the author's doctoral dissertation [24].

Table 2
Controllers coefficients

Variant 1	P	I	λ	D	μ
PID 1	50.40	1.40	—	41.73	—
PID 2	2.87	32.20	—	50.37	—
PID 3	0.23	1.66	—	0.25	—
PID 4	26.89	46.76	—	36.60	—
Variant 2	P	I	λ	D	μ
FOPID 1	44.69	537.13	0.011	40.15	0.99
FOPID 2	16.45	4.63	0.066	162.50	0.70
PID 3	8.27	2.20	—	7.58	—
PID 4	55.10	45.54	—	85.54	—
Variant 3	P	I	λ	D	μ
FOPID 1	261.95	17.95	0.026	21.46	0.99
FOPID 2	3.41	99.94	0.40	24.58	0.88
FOPID 3	18.84	4.52	0.0093	5.54	0.98
FOPID 4	0.26	228.22	0.0022	45.47	0.99

6.1. Simulations

Figure 6 shows the measurement of the azimuth angle with the set value drawn in blue. The first differences can be observed when reaching reference plot. In the case of the third variant, overshoot is visible, while for the first version, a sudden slowdown and slow approach to the set value were noted. After changing reference to an angular value of 0.8 rad overshoots are visible in the first and second variants, greater in the case of the second control version. However, in the first variant, visible oscillations begin to appear in this position.

The behavior of the pitch angle is shown in Fig. 7. It can be observed that when reaching the first maximum, the first and second variants are initially above the reference graph and later (near the maximum) go below. Sudden fluctuations are visible around the 20th and 40th seconds. This is related to the sudden change of the azimuth angle setpoint. The largest deviations are visible for the second variant, the smallest for the first control version.

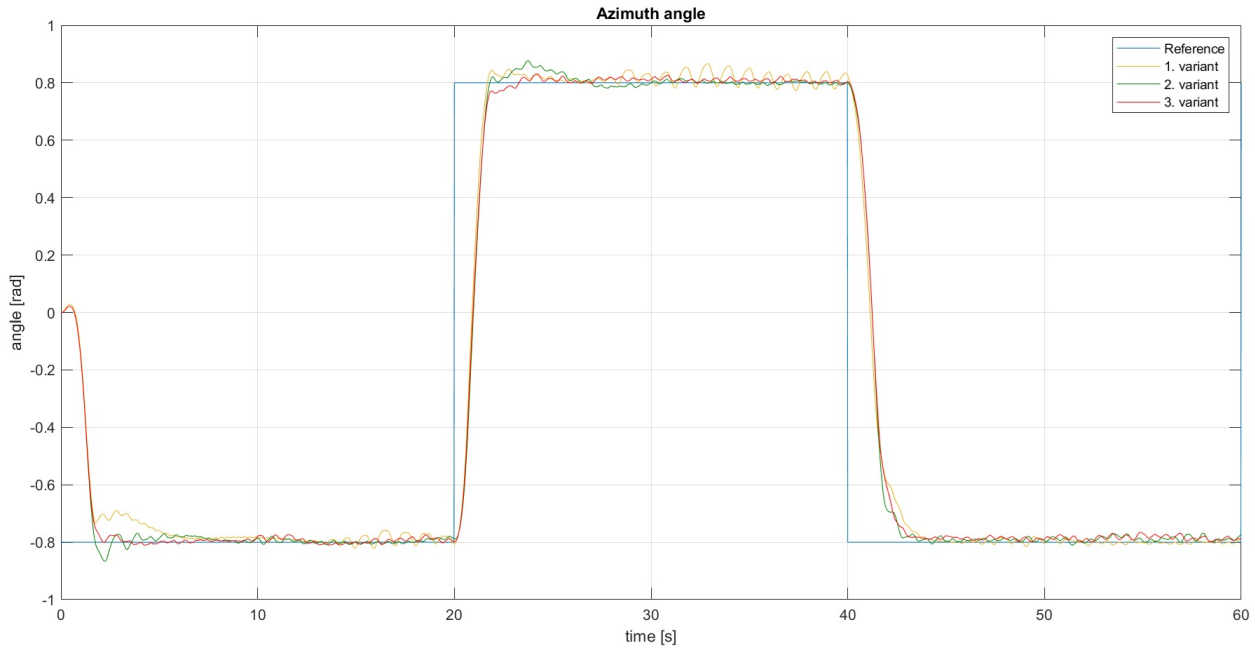

Fig. 6. Simulation system output – azimuth angle

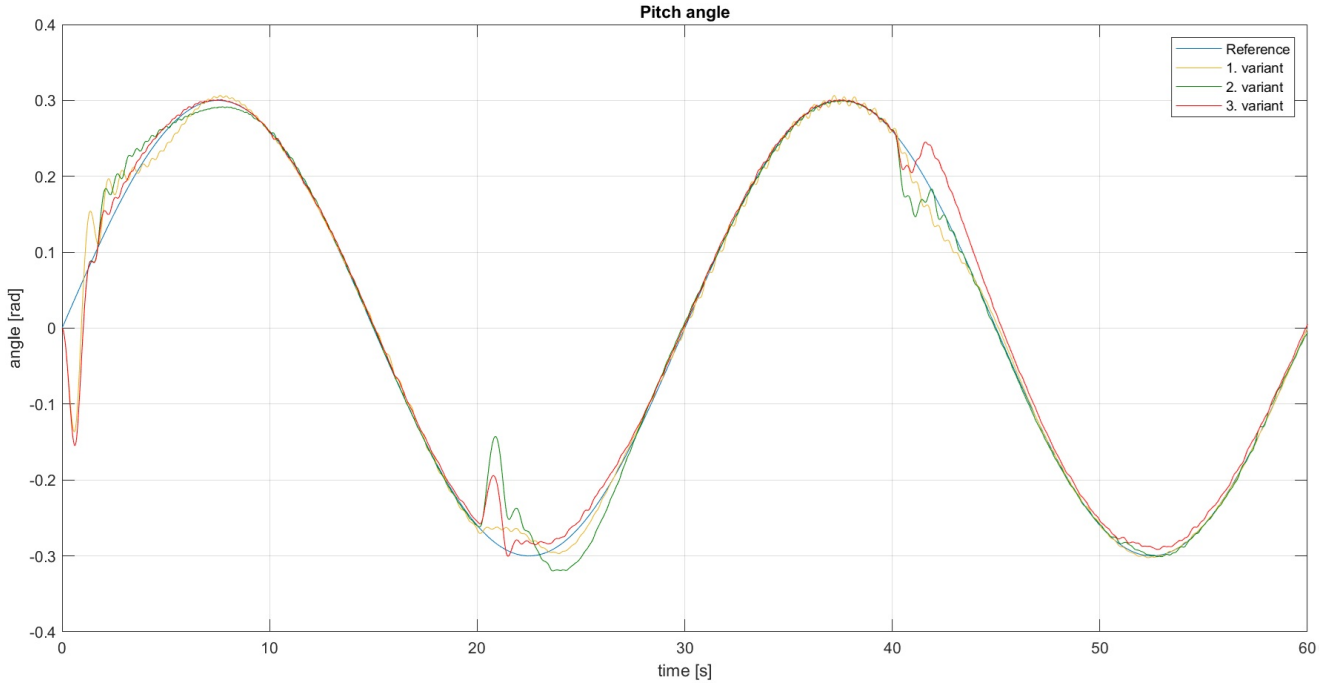

Fig. 7. Simulation system output – pitch angle

Table 3 shows the calculated values of the cost function (17). The second and third variants achieved very similar and better results compared to the first control version. The increased value of the cost function for control with only PIDs was probably caused by the appearance of oscillations for azimuth angle.

Table 3
Values of cost function (17) – simulation

	Value of cost function
Variant 1	303.18
Variant 2	298.76
Variant 3	298.97

6.2. Tests on real object

Figure 8 shows measurements of the azimuth angle from the experiment. It can be seen that the first control version does not reach the reference in the initial phase of measurements. In addition, for a moment it even begins to move away from it. In the case of the second version, two larger overshoots can be seen. The third variant works best. In the case of the upper position for the first control option, overshoot can be observed, which is leveled for a long time. On the other hand, at some point for the second and third variants, noticeable oscillations begin to appear. In the case of the last 20 seconds, all control versions approach very close to the reference, but fail to reach it for a longer period of time.

The graph in Fig. 9 shows the values of the pitch angle measured during the experiment. In the initial phase, very large overshoots can be observed for the first and second variants. In both cases, it is repeated in the opposite direction. However, for the second control option, the attempt to achieve the set value takes longer. In the case of the third variant, a slightly milder approach can be observed, thanks to which the reference area is reached very quickly. After 20 seconds, changes related to the sudden change in the azimuth angle set value are visible. This had the greatest impact on the third control option. On the other hand, the first and second versions behaved in a similar way. Also in the 40th second there was a sudden change in the azimuth angle reference. However, this time the deviations are not as noticeable for all three variants. Additionally, problems with achieving the last minimum can be noted for the second and third control versions.

Table 4 lists the cost function values (17) for the above three experiments. It should be taken into account that the time step this time was 0.01. The lowest value was noted for the third variant. It efficiently achieved the set values of the azimuth and pitch angles. Moreover, in this case, there were fewer overshoots. The only major problem was reaching the extreme values of the reference in the case of the pitch angle.

Table 4
Values of cost function (17) – real object

	Value of cost function
Variant 1	1140.44
Variant 2	1094.05
Variant 3	1064.51

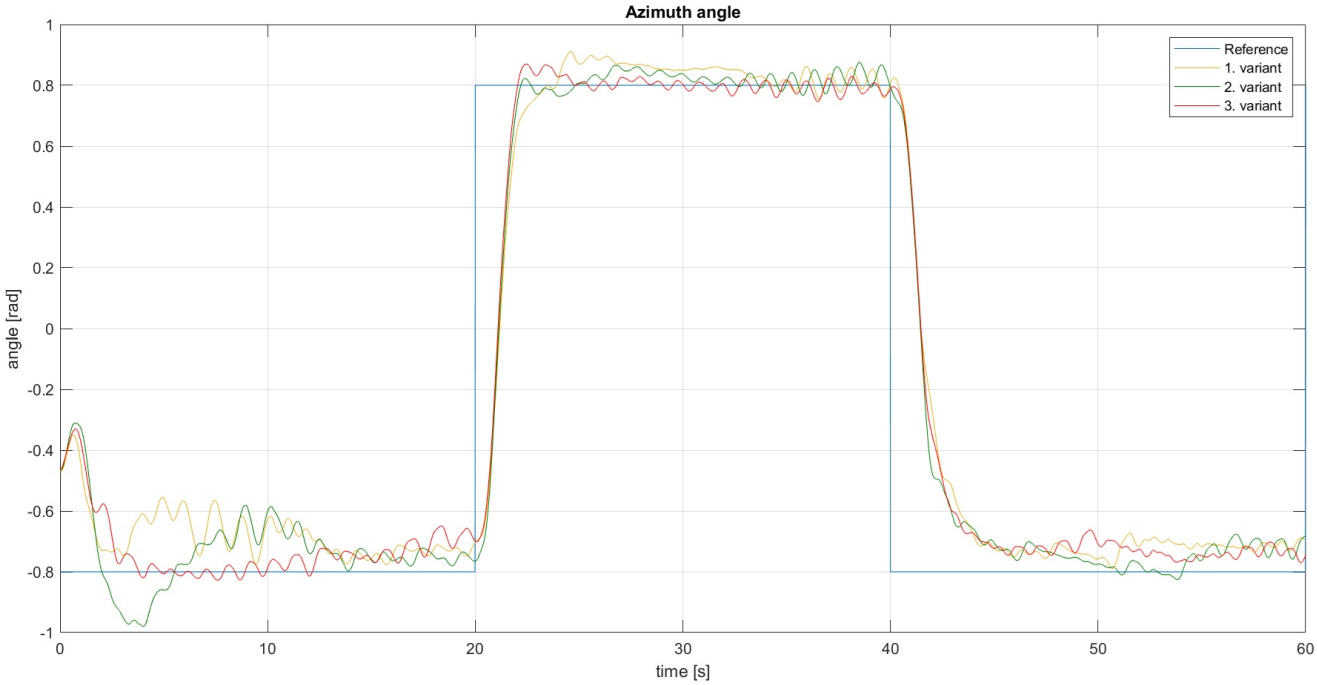

Fig. 8. Real system output – azimuth angle

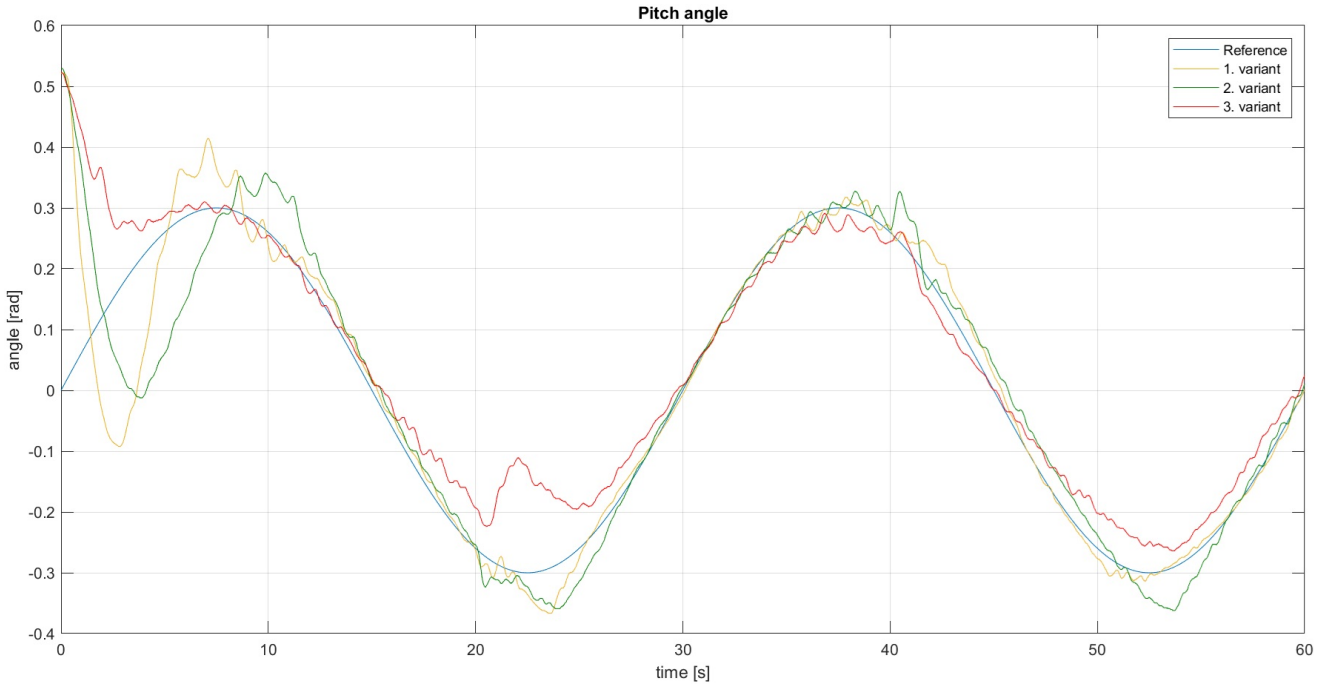

Fig. 9. Real system output – pitch angle

6.3. Calculation times

Figures 10–13 and Table 5 show measurements related to the time of calculations performed by the controllers in the third variant (4 FOPIDs). It can be divided into two sets: FOPID 1 together with FOPID 2 and FOPID 3 together with FOPID 4. In the first case, average times of about 4.6e-07 were recorded, while in the second – 6.2e-07. It is worth noting that the grouping may be related to the calculation for a specific control. For example, FOPID 1 and FOPID 2 controllers calculated the control related to the azimuth rotor. This makes it possible to draw a conclusion that the computer program focused primarily on determining one control in its entirety. The maximum calculation times were at the level of 10^{-6} with a time step of the order of 10^{-2}. Therefore, a large computational reserve was maintained.

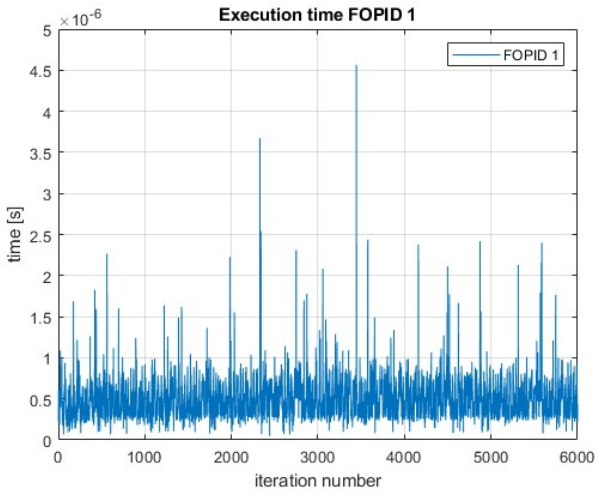

Fig. 10. Execution time – third variant FOPID 1

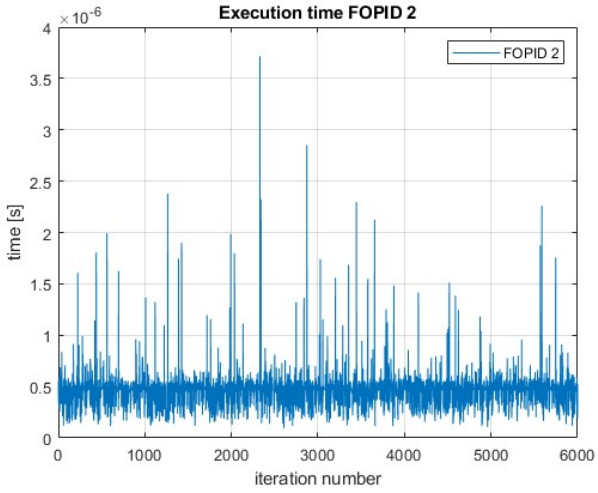

Fig. 11. Execution time – third variant FOPID 2

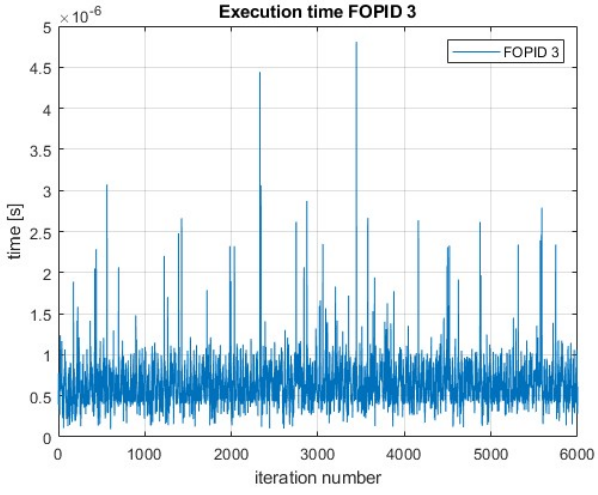

Fig. 12. Execution time – third variant FOPID 3

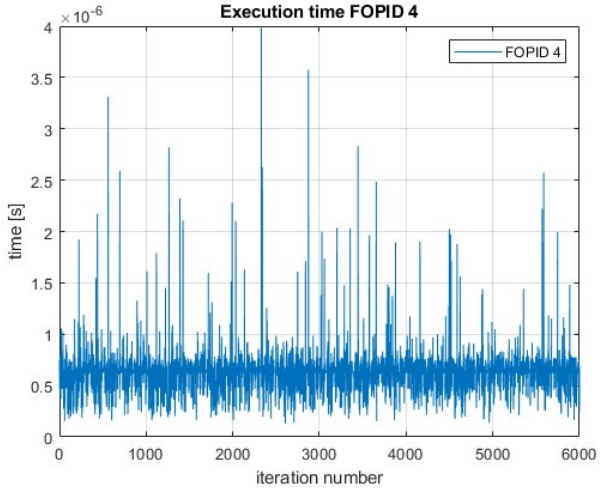

Fig. 13. Execution time – third variant FOPID 4

Table 5

Average and maximum calculation times of controllers – third variant

Controller	Average time [s]	Maximum time [s]
FOPID 1	4.8104e-07	4.5645e-06
FOPID 2	4.5833e-07	3.7158e-06
FOPID 3	6.2919e-07	4.8094e-06
FOPID 4	6.2050e-07	3.9833e-06

7. CONCLUSIONS

Three control versions for Two Rotor Aerodynamical System were prepared, consisting of FOPID and PID controllers. In addition, it was possible to conduct a comparison based on experimental studies. The control in the FOPID version behaved slightly more gently. This allowed for achieving better results. Additionally, the time of performing calculations by the FOPID controllers in the third variant was measured. It turned out that they are fast enough to be used in systems requiring real-time control determination.

More information about the research can be found in the author's doctoral dissertation [24].

In the next article, the author plans to present a similar comparison, but in the case of hybrid control, where in one feedback loop a parallel arrangement of controllers will be used, in the other a cascade. An additional future goal is also to examine the results obtained using other optimization methods.

REFERENCES

[1] S. Zhao, K. Lu, S. Wu, and D. Su, "Helicopter Flight Dynamics Modeling Using Simulink," in *2021 33rd Chinese Control and Decision Conference (CCDC)*, 2021, pp. 2591–2596, doi: 10.1109/CCDC52312.2021.9601647.

[2] Z. Domozi and A. Molnar, "Surveying private pools in suburban areas with neural network based on drone photos," in *IEEE EUROCON 2019 – 18th International Conference*

on Smart Technologies, 2019, pp. 1–6, doi: 10.1109/EUROCON.2019.8861770.

[3] T. Arai, K. Iwata, K. Hara, and Y. Satoh, "Estimation of Human Condition at Disaster Site Using Aerial Drone Images," in *2023 IEEE/CVF International Conference on Computer Vision Workshops (ICCVW)*, 2023, pp. 3777–3785, doi: 10.1109/ICCVW60793.2023.00408.

[4] P. Daponte, L. De Vito, F. Lamonaca, F. Picariello, S. Rapuano, and M. Riccio, "Measurement science and education in the drone times," in *2017 IEEE International Instrumentation and Measurement Technology Conference (I2MTC)*, 2017, pp. 1–6, doi: 10.1109/I2MTC.2017.7969979.

[5] N. Karna, A. Salsabilla, and S. Y. Shin, "Automatic Take Off and Landing (ATOL) Towards Internet of Drone Things for Air Quality Measurement," in *2024 15th International Conference on Information and Communication Technology Convergence (ICTC)*, 2024, pp. 327–331, doi: 10.1109/ICTC62082.2024.10827810.

[6] INTECO, *Two Rotor Aero-dynamical System User's Manual*. Inteco Sp. z o.o., 2010.

[7] V. Mihaly, M. Şuşcă, and E.H. Dulf, "μ-Synthesis FO-PID for Twin Rotor Aerodynamic System," *Mathematics*, vol. 9, no. 19, p. 2504, 2021, doi: 10.3390/math9192504.

[8] S. Al-Haddad and H. Wahid, "Decoupled integral lqr controller with anti-windup compensator for mimo two rotor aerodynamical system (TRAS)," *J. Eng. Sci. Technoll*, vol. 14, no. 3, p. 1374–1397, 2019. [Online]. Available: https://www.scopus.com/pages/publications/85072062034

[9] N. Minorsky, "Directional stability of automatically steered bodies," *J. Am. Soc. Naval Eng.*, vol. 34, no. 2, pp. 280–309, 1922, doi: 10.1111/j.1559-3584.1922.tb04958.x.

[10] P. Abinaya, R. Muniraj, S. Amritha, and M. Sivapalanirajan, "Performance Comparison of MPC and PID Controller for Single Input Single Output Process," in *2019 International Conference on Recent Advances in Energy-efficient Computing and Communication (ICRAECC)*, 2019, pp. 1–6, doi: 10.1109/ICRAECC43874.2019.8995011.

[11] L.M. Argentim, W.C. Rezende, P.E. Santos, and R.A. Aguiar, "PID, LQR and LQR-PID on a quadcopter platform," in *2013 International Conference on Informatics, Electronics and Vision (ICIEV)*, 2013, pp. 1–6, doi: 10.1109/ICIEV.2013.6572698.

[12] A.F. Al-Saoudi, K.M. Al-Aubidy, and A.J. Al-Mahasneh, "Comparison of PID, Fuzzy Logic, ANFIS and Model Predictive Controllers for Cruise Control System," in *2024 21st International Multi-Conference on Systems, Signals & Devices (SSD)*, 2024, pp. 263–265, doi: 10.1109/SSD61670.2024.10548200.

[13] A. Kilbas, H. Srivastava, and J. Trujillo, *Theory and Applications of Fractional Differential Equations*, ser. North-Holland Mathematics Studies. Elsevier Science, 2006. [Online]. Available: https://www.sciencedirect.com/bookseries/north-holland-mathematics-studies/vol/204/suppl/C

[14] P. Ostalczyk, *Discrete Fractional Calculus: Applications In Control And Image Processing*, ser. Series In Computer Vision. World Scientific Publishing Company, 2015. [Online]. Available: https://books.google.pl/books?id=A2LFCwAAQBAJ

[15] S. Mirjalili, S. M. Mirjalili, and A. Lewis, "Grey Wolf Optimizer," *Adv. Eng. Softw.*, vol. 69, pp. 46–61, 2014, doi: 10.1016/j.advengsoft.2013.12.007.

[16] S. Mirjalili and A. Lewis, "The Whale Optimization Algorithm," *Adv. Eng. Softw.*, vol. 95, pp. 51–67, 2016, doi: 10.1016/j.advengsoft.2016.01.008.

[17] J. Kennedy and R. Eberhart, "Particle swarm optimization," in *Proceedings of ICNN'95 – International Conference on Neural Networks*, vol. 4, pp. 1942–1948, 1995, doi: 10.1109/ICNN.1995.488968.

[18] A. Ahmed, G. Parmar, and R. Gupta, "Application of GWO in Design of Fractional Order PID Controller for Control of DC Motor and Robustness Analysis," in *2018 International Conference on Advances in Computing, Communication Control and Networking (ICACCCN)*, 2018, pp. 646–651, doi: 10.1109/ICACCCN.2018.8748548.

[19] D. Mazumdar, P.K. Biswas, C. Sain, F. Ahmad, and L. Al-Fagih, "A comprehensive analysis of the optimal GWO based FOPID MPPT controller for grid-tied photovoltaics system under atmospheric uncertainty," *Energy Rep.*, vol. 12, pp. 1921–1935, 2024, doi: 10.1016/j.egyr.2024.08.013.

[20] R. Caponetto, G. Dongola, L. Fortuna, and I. Petras, *Fractional Order Systems: Modeling And Control Applications*, ser. World Scientific Series On Nonlinear Science Series A. World Scientific Publishing Company, 2010. [Online]. Available: https://books.google.pl/books?id=ULbFCgAAQBAJ

[21] A. Oustaloup, F. Levron, B. Mathieu, and F.M. Nanot, "Frequency-band complex noninteger differentiator: characterization and synthesis," *IEEE Trans. Circ. Syst. I-Fundam. Theor. Appl.*, vol. 47, no. 1, pp. 25–39, 2000, doi: 10.1109/ 81.817385.

[22] I. Podlubny, "Fractional-order systems and $PI^{\lambda}D^{\mu}$-controllers," *IEEE Transactions on Automatic Control*, vol. 44, no. 1, pp. 208–214, 1999, doi: 10.1109/9.739144.

[23] I. Podlubny, I. Petráš, B.M. Vinagre, P. O'Leary, and Ľ. Dorčák, "Analogue Realizations of Fractional-Order Controllers," *Nonlinear Dyn.*, vol. 29, no. 1, pp. 281–296, Jul 2002, doi: 10.1023/A:1016556604320.

[24] J. Żegleń Włodarczyk, "Szybkie sterowanie niecałkowitego rzędu obiektami nieliniowymi," PhD thesis, AGH University of Krakow, 2024. [Online]. Available: https://www.eaiib.agh.edu.pl/wp-content/uploads/2024/02/ZEGLEN-WLODARCZYK-JAKUB_ROZPRAWA-DOKTORSKA.pdf